A Simplified Analysis of Resonant Extraction at the Main Injector

John A. Johnstone
Fermi National Accelerator Lab
September 3, 1993

Introduction

At the Main Injector slow extraction proceeds via excitation of the half-integer resonance. Quadrupoles distributed on the 53^{rd}-harmonic provide the half-integer driving term, while octupoles distributed around the ring excite the 0^{th}-harmonic. The (non-linear) octupole field produces an amplitude-dependent tune-shift ($\Delta\nu \propto x^2$), with larger amplitude particles having tunes closer to the half-integer. Consequently, the phase-space splits into stable and unstable regions. Ramping the harmonic quadrupoles increases the width of the half-integer stop-band. As the area of the stable region shrinks to the point that it no longer encompasses the beam emittance, large amplitude particles become unstable and stream out along the separatrices.

The primary concern in design of the extraction system is to achieve an acceptable compromise between the two conflicting processes of minimizing extracted beam emittance and maximizing extraction efficiency. Machine aperture limitations, in addition, constrain the maximum permissable amplitude for the circulating beam. The non-linear nature of the resonance guarantees that these characteristics are inter-dependent functions of the extraction parameters: these being; the strengths of harmonic quadrupole and octupole circuits, the effective betatron phase difference between the harmonic quadrupoles and septum, the septum offset, and the initial tune separation from the half-integer.

It is precisely because slow extraction is a non-linear phenomenon that numerical tracking codes are *not* the appropriate tools for initial exploration of the parameter space. The degree of true insight into the system dynamics obtainable by such an approach is severely limited. The number of particles that can be conveniently tracked (typically ~ 1000) is sufficiently small that details of the system response are masked by statistical variations. Furthermore, tracking is limited to, perhaps, a few thousand turns, which does not provide a particularly good approximation to the adiabatic slow extraction process.

It is the intent in this note to demonstrate that analytic exploration of the system dynamics can quickly narrow the range of acceptable parameters. First, Hamilton's equations of motion in the presence of perturbing quadrupole and octupole fields are given. In subsequent sections the step-size at the septum, maximum circulating beam amplitude, extracted beam emittance, and extraction inefficiency are derived under the conditions which exist at the end of extraction; that is, when there is zero stable phase-space area. This simplification does not qualitatively alter the conclusions one obtains from the general case, but the resulting equations lend themselves more readily to transparent interpretation. (Detailed general results will be presented elsewhere[1]). The concluding sections discuss the selection of the extraction parameters, and compares analytic prediction with results obtained from numerical simulation.

General Equations of Motion

For isolated resonances, the motion of a particle in transverse phase-space can be represented by an idealized Hamiltonian, $\hat{H}$, which is an approximate constant of the motion. Near the half-integer, with only 0^{th}-harmonic octupole and 53^{rd}-harmonic quadrupole perturbations, $\hat{H}$ can be written as:

$$\hat{H} = [\delta - \hat{q}cos(2\phi - \chi)]\, R^2 - 3\hat{\lambda}R^4 \tag{1}$$

For simplicity, momentum-dependent effects and coupling between the tranverse planes have been neglected. The linear betatron phase advance $\hat{\theta} \equiv \int ds/\nu\beta$ is conjugate to $\hat{H}$. Other variables are: the fractional tune separation;

$$\delta = (53/2 - \nu) \tag{2}$$

and the action-angle variables, R^2 and ϕ;

$$\beta R^2 = x^2 + (\beta p + \alpha x)^2 \; ; \; \phi = \frac{53}{2}\hat{\theta} + tan^{-1}[(\beta p + \alpha x)/x] \tag{3}$$

The half-integer driving term $\hat{q}$ is defined as $\hat{q} \equiv [q_S^2 + q_C^2]^{1/2}$, where q_S and q_C are the orthogonal sine and cosine-like quadrupole contributions:

$$q_S \;=\; \frac{1}{2\pi}\oint ds \frac{B'\beta}{2B_0\rho} \cdot sin(53\hat{\theta}) \; ; \; q_C = \frac{1}{2\pi}\oint ds \frac{B'\beta}{2B_0\rho} \cdot cos(53\hat{\theta}) \tag{4}$$

[1] elsewhere: not here.

The angle χ determines the orientation of the phase-space at the septum:

$$\chi \equiv tan^{-1}\left[q_S/q_C\right] \tag{5}$$

The 0^{th}-harmonic term $\hat{\lambda}$ is the integral of the octupole field around the ring:

$$\hat{\lambda} = \frac{1}{2\pi}\oint ds \frac{B'''\beta^2}{96B_0\rho} \tag{6}$$

In the interests of brevity of notation, it is convenient to change the normalization of the Hamiltonian. First, $\hat{H}$ is rescaled to $H \equiv \hat{H}/\delta$, and the new conjugate variable becomes $\theta \equiv \delta\hat{\theta}$, which advances by $2\pi\delta$ per turn. The explicit dependence on the octupole field $\hat{\lambda}$ can be removed by rescaling the transverse action co-ordinate R^2 to $r^2 \equiv (6\hat{\lambda}/\delta)\cdot R^2$. With these revisions the Hamiltonian becomes:

$$\kappa = \left[1 - qcos(2\phi - \chi)\right] r^2 - r^4/2 \tag{7}$$

Now $\kappa \equiv (6\hat{\lambda}/\delta)H$ is the approximate constant of the motion, and $q \equiv \hat{q}/\delta$. In this normalization $q \rightarrow 1$ in the limit of zero stable phase-space.

Hamilton's equations of motion are determined from (7):

$$\begin{aligned} \frac{dr^2}{d\theta} &= -\frac{\partial\kappa}{\partial\phi} = -2qr^2 sin(2\phi - \chi) \\ \frac{d\phi}{d\theta} &= +\frac{\partial\kappa}{\partial r^2} = \left[1 - qcos(2\phi - \chi)\right] - r^2 \end{aligned} \tag{8}$$

The fixed points are those values for which eqns.(8) are zero:

$$2\phi_F - \chi = 0, \pi, 2\pi, 3\pi \tag{9}$$

The unstable fixed points are $0, 2\pi$, or $\phi_F = \chi/2$, and $\pi + \chi/2$. Stable fixed points are located at π and 3π. At the unstable fixed points:

$$r_F^2 = \left[1 - qcos(2\phi_F - \chi)\right] \rightarrow (1 - q) \tag{10}$$

and $r_F^2 \rightarrow (1 + q)$ at the stable points. The existence of the two stable fixed points at large radii means that all phase-space contours of constant $\hat{H}$ are, in fact, closed. However these points are so far from the origin that, for the purposes of the current discussion, the separatrices are effectively unbounded.

From eqns.(7)-(10) the separatrices in general therefore satisfy:

$$r^4 - 2\left[1 - qcos(2\phi - \chi)\right] r^2 - (1-q)^2 = 0 \tag{11}$$

or, equivalently:

$$\left[r^2 - 2\sqrt{q}sin(\phi - \chi/2)r - (1-q)\right]\left[r^2 + 2\sqrt{q}sin(\phi - \chi/2)r - (1-q)\right] = 0$$

This is the description of two overlapping circles of unit radii. This is most clearly seen by rewriting the equation in terms of normalized phase-space variables $\hat{x}$ and $\hat{x}'$, related to r and ϕ at the septum by $\hat{x}$ $[\hat{x}'] \equiv rcos(\phi)$ $[rsin(\phi)]$. The two curves describing the separatrices then take the form:

$$\left[\hat{x} \pm \sqrt{q}sin(\chi/2)\right]^2 + \left[\hat{x}' \mp \sqrt{q}cos(\chi/2)\right]^2 = 1 \tag{12}$$

The fixed points in this notation are given by the intersection of the two circles:

$$(\hat{x}_F, \hat{x}'_F) = \left[\pm\sqrt{1-q}\cdot cos(\chi/2), \pm\sqrt{1-q}\cdot sin(\chi/2)\right] \tag{13}$$

The stable phase-space region is the area enclosed by the overlap of the two circles. Extraction begins when q and λ are such that the stable region has shrunk to the point that it equals the emittance of the circulating beam:

$$\pi\epsilon = \frac{\delta}{3\hat{\lambda}}\left\{sin^{-1}[\sqrt{1-q}] - \sqrt{q}\sqrt{1-q}\right\} \tag{14}$$

The generally high quality of the Hamiltonian description is apparent from Fig.1, which compares representative contours of constant $\hat{H}$. The upper diagram shows predicted contours for (normalized) emittances of $\pi\epsilon_N = 10, 30, 90,$ and 270π-mm-mr. The lower diagram shows the corresponding results from numerically tracking particles initially launched with these values. The harmonic quadrupole strength $\hat{q}$ is such that the 30π contour is the stability limit. The other relevant parameters (δ, λ, and χ) are values appropriate to the Main Injector. (The selection of these parameters is, of course, the subject of subsequent sections). The evolution of a typical contour as the stop-band width ($\hat{q}$) is increased during extraction is shown in Fig.2.

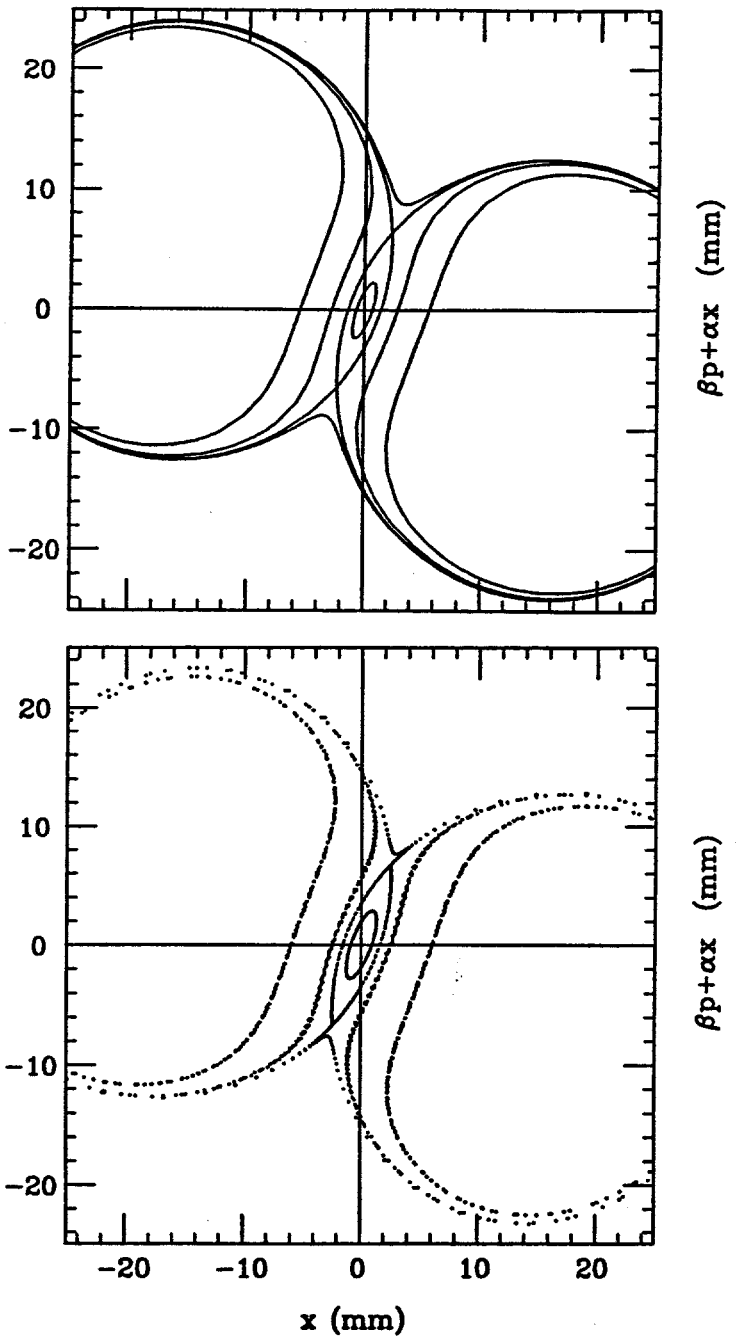

Figure 1: Comparison of representative contours of constant $\hat{H}$. The upper diagram shows predicted contours for $\pi\epsilon_N = 10, 30, 90$, and 270π-mm-mr, while the lower diagram results from numerical tracking. The innermost contour is stable. The next is the stability limit with fixed points at the intersections of the circles. The remaining contours are unstable.

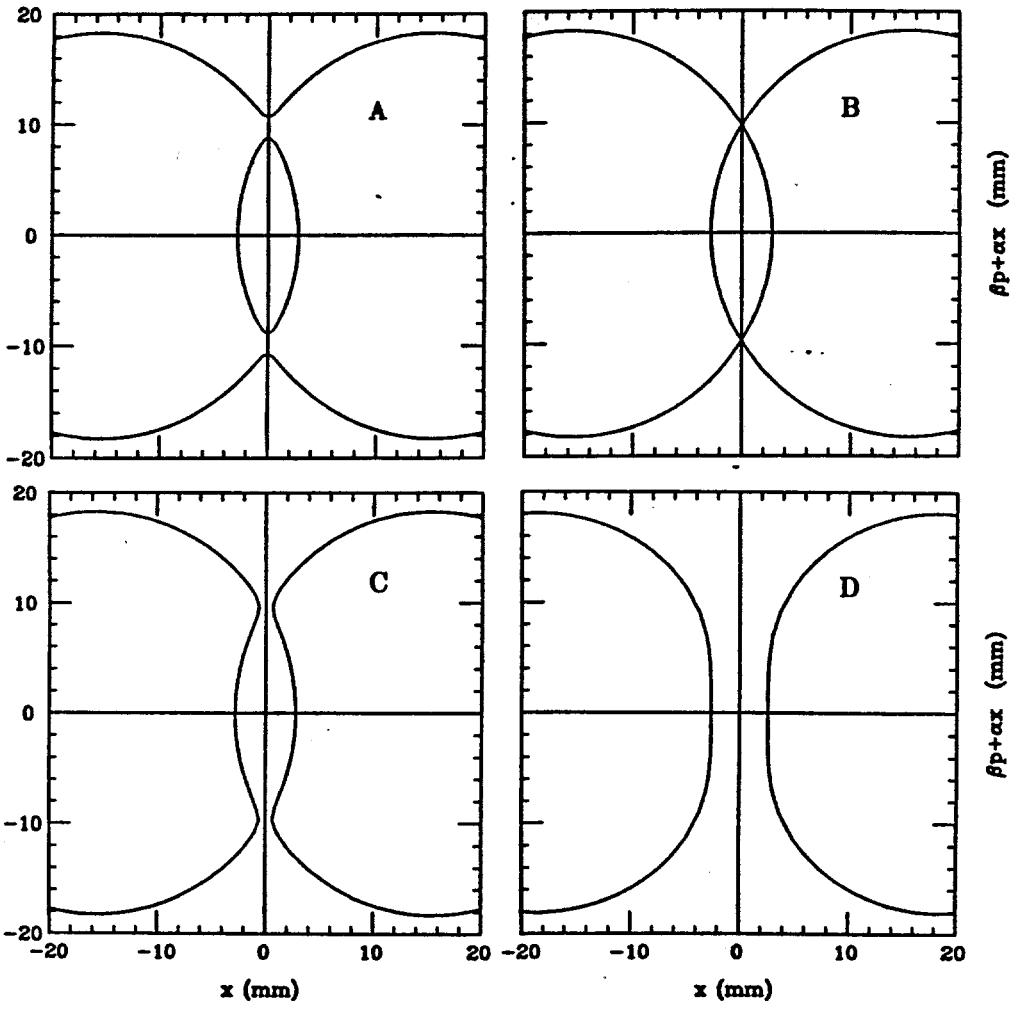

Figure 2: Evolution of a typical contour during extraction: a) central stable and outer unstable contours are unconnected; b) stability limit, with the stable region given by the overlap of the circles; c) both contours are unstable, and; d) at the end of extraction ($\hat{q} = \delta$).

Step-Size at the Septum

Given values of δ, λ, and the septum offset; extraction efficiency, extracted emittance, and maximum amplitude of the circulating beam are determined by the step-size at the septum. Since the separatrix is a circle of unit radius, the motion of particles in $\hat{x} - \hat{x}'$ space can be described by an angle of rotation about the circle center. At the end of extraction ($q = 1$) the angle η is:

$$\begin{aligned} \hat{x} - sin(\chi/2) &= -cos(\eta) \\ \hat{x}' + cos(\chi/2) &= +sin(\eta) \end{aligned} \tag{15}$$

This co-ordinate system is depicted in Fig.3.

The two-turn increase $\Delta\eta$ in η is found by first differentiating eqns.(15):

$$\begin{aligned} sin(\eta)\frac{d\eta}{d\theta} &= \frac{d\hat{x}}{d\theta} = -rsin(\phi)\cdot\frac{d\phi}{d\theta} + cos(\phi)\cdot\frac{dr}{d\theta} \\ &= 2\,[\hat{x}' + cos(\chi/2)]\,[\hat{x}sin(\chi/2) - \hat{x}'cos(\chi/2)] \\ \Rightarrow \frac{d\eta}{d\theta} &= 2\,[1 - sin(\eta + \chi/2)] \end{aligned} \tag{16}$$

where the final line follows from the definitions (15). The increase $\Delta\eta$ in η_0 is then solved from the integral equation:

$$\int_{\eta_0}^{\eta_0+\Delta\eta} \frac{d\eta}{2\,[1 - sin(\eta + \chi/2)]} = 4\pi\delta \tag{17}$$

where the right-hand side results from θ advancing by $4\pi\delta$ in two turns.

The solution to (17) is straightforward:

$$\Delta\eta = 2\cdot tan^{-1}\left\{\frac{4\pi\delta\cdot[1 - sin(\eta_0 + \chi/2)]}{1 + 4\pi\delta\cdot cos(\eta_0 + \chi/2)}\right\} \tag{18}$$

The initial tune separation δ from the half-integer is a small number $\ll 1$ ($\delta = .015$ at the Injector, for example). It is a good approximation therefore to expand the right-hand side of the above equation to first-order in δ:

$$\Delta\eta \approx 8\pi\delta\cdot[1 - sin(\eta_0 + \chi/2)] \tag{19}$$

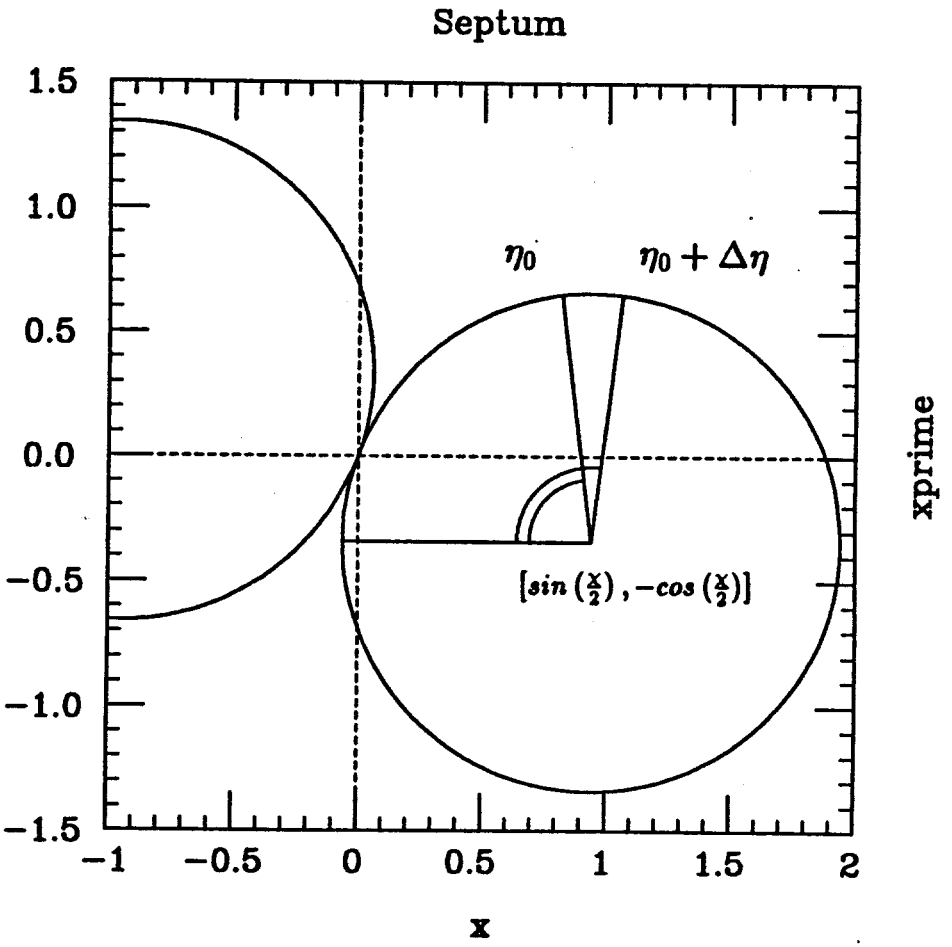

Figure 3: Motion of a particle in normalized $\hat{x} - \hat{x}'$ space in terms of the angle η. The septum is at η_0. The step-size at the septum is $\Delta\eta$.

Maximum Amplitude of Circulating Beam

Aperture restrictions (physical or dynamic) limit the maximum amplitude permissable for the circulating beam. Referring to Fig.3, the amplitude at the septum is the distance from the origin ($\eta = \pi/2 - \chi/2$) to the point $\eta = \eta_0 + \Delta\eta$. If β_{max} is the largest betatron amplitude in the machine, then the maximum amplitude is simply:

$$a_{max} = \sqrt{\frac{\delta\beta_{max}}{6\lambda}} \cdot 2sin\left[\frac{1}{2}\left(\eta_0 + \Delta\eta - \frac{\pi}{2} + \frac{\chi}{2}\right)\right] \tag{20}$$

Extracted Beam Emittance

The emittance of the extracted beam can be defined in two (inequivalent) ways. Extracted particles fall essentially along a straight line in phase-space. During the course of extraction, however, the step-size and orientation at the septum varies slightly so that the line becomes broadened. This area swept out by the particles is the usual definition of extracted beam emittance encountered in the literature. However, this quantity can be a misleadingly small number and great care must be taken in its interpretation to avoid possible aperture problems in the extraction beamline. An alternative which avoids this complication (and the definition employed here) is to define extracted emittance as the area of the smallest phase-space circle that encompasses all the particles. In other words, extracted beam emittance is defined equivalently to a circulating beam.

The radius of the smallest circle enclosing the extracted beam (refer to Fig.3) is $sin(\Delta\eta/2)$. The extracted emittance is therefore:

$$\pi\epsilon = \frac{\delta}{6\lambda}\pi \cdot [sin(\Delta\eta/2)]^2 \tag{21}$$

Extraction Inefficiency

Extraction inefficiency is defined as the fraction of particles that are lost by hitting the septum wires relative to the number that are extracted. The density of particles at any point along the outgoing separatrix is inversely proportional to the streaming speed at that point. If it is assumed that all particles hitting

using the results of eqns.(16)-(18), and expressed as:

$$f = \frac{\int_{\hat{x}_0}^{\hat{x}_0+\hat{\omega}} d\hat{x}/\left(d\hat{x}/d\theta\right)}{\int_{\hat{x}_0}^{\hat{x}_0+\Delta} d\hat{x}/\left(d\hat{x}/d\theta\right)} \tag{22}$$

The denominator is the total number of particles extracted. The finite upper limit of integration reflects the fact that the maximum value of $\hat{x}$ is limited by the step-size at the septum. From eqn.(17) the denominator is $4\pi\delta$. The numerator is the relative number of particles striking the wire of width $\hat{\omega}$. The normalized width $\hat{\omega}$ is related to the physical width w by $\hat{\omega} = \sqrt{6\lambda/\delta\beta} \cdot w$. For a thin wire $d\hat{x}/d\theta$ does not vary appreciably across the width so that it can be removed from under the integral sign, with the result:

$$f = \frac{\hat{\omega}}{8\pi\delta \cdot sin(\eta_0)\left[1 - sin(\eta_0 + \chi/2)\right]} \tag{23}$$

Using the approximation (19) for $\Delta\eta$, and noting that $sin(\eta_0) \approx 1$ always, the inefficiency can be written in terms of the step-size as approximately:

$$f \approx \sqrt{\frac{3\lambda}{2\delta\beta}} \cdot \frac{\omega}{sin\left(\Delta\eta/2\right)} \tag{24}$$

Comparing the above expression for f with extracted emittance (21) leads to the remarkable relationship:

$$f \approx \frac{\omega}{2\sqrt{\beta\epsilon}} \tag{25}$$

Extraction efficiency can only be improved at the expense of blowing up the extracted emittance. This in itself is not surprising, but eqn.(25) claims that, at least to first order, the relationship between inefficiency and emittance is independent of octupole strength, phase-angle χ, initial tune separation δ, and septum offset! For a given value of emittance the only parameters that affect efficiency are the wire width ω and amplitude β at the septum.

Septum Offset

The Injector MI-52 straight section must accomodate a variety of extraction and injection scenarios. It is desireable, therefore, to minimize the slow-extracted beam size at the extraction Lambertson. For a Lambertson located 90° in

betatron phase dowstream of the septum, it is clear from Fig.3 that this will be accomplished if the angle η_0 is chosen such that:

$$\begin{aligned} sin(\eta_0) &= sin(\eta_0 + \Delta\eta) \\ \Rightarrow \eta_0 &= \frac{\pi}{2} - \frac{\Delta\eta}{2} \end{aligned} \tag{26}$$

With this simplification eqn.(18) can be rewritten to express the step-size $\Delta\eta$ exclusively as a function of the angle χ and tune separation δ:

$$\Delta\eta = 2 \cdot sin^{-1}\left\{\frac{4\pi\delta}{1+(4\pi\delta)^2}\left[-cos(\chi/2) + \sqrt{1+[4\pi\delta sin(\chi/2)]^2}\right]\right\} \tag{27}$$

Perusing Parameter Space

With step-size related to septum offset η_0 by eqn.(26), the other relevant extraction properties can be simplified to:

$$x_{sep} = \sqrt{\frac{\delta\beta_{sep}}{6\lambda}} \cdot [sin\,(\chi/2) - sin\,(\Delta\eta/2)] \tag{28}$$

$$a_{max} = \sqrt{\frac{\delta\beta_{max}}{3\lambda}} \cdot [1 - cos\,(\Delta\eta/2 + \chi/2)]^{1/2} \tag{29}$$

$$\pi\epsilon = \frac{\pi\delta}{6\lambda} \cdot [sin\,(\Delta\eta/2)]^2 \tag{30}$$

$$f = \sqrt{\frac{6\lambda}{\delta\beta_{sep}}} \cdot \frac{\omega}{8\pi\delta \cdot cos\,(\Delta\eta/2)\,[1 - cos\,(\Delta\eta/2 - \chi/2)]} \tag{31}$$

The variation of maximum beam amplitude, emittance, and inefficiency with the extraction parameters can be explored as follows: given an initial tune separation δ and harmonic phase $\chi/2$, step-size at the septum is defined by eqn.(27), and; given a value for the septum offset x_{sep}, the octupole strength λ required is fixed by condition (28). There are no remaining free parameters at this point and a_{max}, $\pi\epsilon$, and f are completely defined. Variation of δ, x_{sep}, and $\chi/2$ then spans the parameter space. Table 1 illustrates this procedure for tune separation $\delta = .020$, septum offsets of 14, 16, and 18 mm, and appropriate values of $\chi/2$. Tables 2 and 3 repeat the procedure for $\delta = .015$ and .010.

Septum Offset = 14.0 mm				
$\chi/2$ ^{0}	λ m^{-1}	a_{max} mm	$\pi\epsilon_N$ π-mm-mr	f %
40.	209	22.8	6.9	4.21
45.	246	23.7	9.2	3.72
50.	281	24.7	12.0	3.31
55.	312	25.7	15.3	2.97
60.	337	26.9	19.3	2.68
65.	357	28.2	24.3	2.42
70.	370	29.7	30.2	2.19
75.	376	31.3	37.6	1.99
80.	375	33.1	46.6	1.80
Septum Offset = 16.0 mm				
$\chi/2$ ^{0}	λ m^{-1}	a_{max} mm	$\pi\epsilon_N$ π-mm-mr	f %
40.	160	26.1	9.1	3.68
45.	189	27.1	12.0	3.25
50.	215	28.2	15.6	2.90
55.	239	29.4	20.0	2.60
60.	258	30.8	25.3	2.34
65.	273	32.2	31.7	2.12
70.	283	33.9	39.5	1.92
75.	288	35.8	49.1	1.74
80.	287	37.9	60.9	1.58
Septum Offset = 18.0 mm				
$\chi/2$ ^{0}	λ m^{-1}	a_{max} mm	$\pi\epsilon_N$ π-mm-mr	f %
40.	126	29.4	11.5	3.27
45.	149	30.5	15.2	2.89
50.	170	31.7	19.8	2.58
55.	188	33.1	25.3	2.31
60.	204	34.6	32.0	2.08
65.	216	36.3	40.1	1.88
70.	224	38.1	50.0	1.71
75.	228	40.2	62.1	1.55
80.	227	42.6	77.1	1.40

Table 1: Variation of octupole strength, maximum circulating beam amplitude, (normalized) extracted emittance, and extraction inefficiency as a function of the harmonic phase angle $\chi/2$ and septum offset. β_{sep} = 36 m, β_{max} = 60 m, ω = 0.1 mm, and initial tune separation from the half-integer δ = .020.

Septum Offset = 14.0 mm				
$\chi/2$ °	λ m^{-1}	a_{max} mm	$\pi\epsilon_N$ π-mm-mr	f %
50.	224	23.4	6.4	4.32
55.	251	24.3	8.1	3.87
60.	274	25.3	10.2	3.49
65.	293	26.3	12.7	3.16
70.	307	27.6	15.7	2.86
75.	315	28.9	19.3	2.59
80.	317	30.4	23.8	2.35
85.	314	32.2	29.2	2.13
90.	305	34.2	36.0	1.93
Septum Offset = 16.0 mm				
$\chi/2$ °	λ m^{-1}	a_{max} mm	$\pi\epsilon_N$ π-mm-mr	f %
50.	172	26.8	8.3	3.78
55.	192	27.8	10.6	3.39
60.	210	28.9	13.3	3.05
65.	224	30.1	16.6	2.76
70.	235	31.5	20.5	2.50
75.	241	33.0	25.2	2.27
80.	243	34.8	31.0	2.06
85.	240	36.8	38.1	1.87
90.	233	39.0	47.0	1.69
Septum Offset = 18.0 mm				
$\chi/2$ °	λ m^{-1}	a_{max} mm	$\pi\epsilon_N$ π-mm-mr	f %
50.	136	30.1	10.5	3.36
55.	152	31.2	13.4	3.00
60.	166	32.5	16.8	2.71
65.	177	33.9	21.0	2.45
70.	185	35.4	25.9	2.22
75.	190	37.2	31.9	2.02
80.	192	39.1	39.3	1.83
85.	190	41.4	48.3	1.66
90.	184	43.9	59.5	1.50

Table 2: Same description as Table 1, but with $\delta = .015$

Septum Offset = 14.0 mm				
$\chi/2$ ^{0}	λ m^{-1}	a_{max} mm	$\pi\epsilon_N$ π-mm-mr	f %
60.	198	23.7	4.2	5.12
65.	213	24.6	5.2	4.63
70.	225	25.6	6.4	4.20
75.	233	26.7	7.8	3.82
80.	238	27.9	9.5	3.47
85.	238	29.4	11.6	3.16
90.	235	31.0	14.1	2.86
95.	227	32.8	17.2	2.60
100.	215	35.0	21.1	2.34
Septum Offset = 16.0 mm				
$\chi/2$ ^{0}	λ m^{-1}	a_{max} mm	$\pi\epsilon_N$ π-mm-mr	f %
60.	151	27.1	5.5	4.48
65.	163	28.1	6.8	4.05
70.	172	29.2	8.4	3.68
75.	179	30.5	10.2	3.34
80.	182	31.9	12.5	3.04
85.	182	33.6	15.2	2.76
90.	180	35.4	18.5	2.51
95.	174	37.5	22.5	2.27
100.	165	40.0	27.6	2.05
Septum Offset = 18.0 mm				
$\chi/2$ ^{0}	λ m^{-1}	a_{max} mm	$\pi\epsilon_N$ π-mm-mr	f %
60.	120	30.5	7.0	3.98
65.	129	31.6	8.6	3.60
70.	136	32.9	10.6	3.27
75.	141	34.3	12.9	2.97
80.	144	35.9	15.8	2.70
85.	144	37.7	19.2	2.45
90.	142	39.8	23.4	2.23
95.	137	42.2	28.5	2.02
100.	130	44.9	34.9	1.82

Table 3: Same description as Table 1, but with δ = .010

From the preceding tables [and eqns.(28)-(31)] some general features are evident:

- For fixed δ, $\chi/2$, and increasing septum offset:
  1. octupole field strength required decreases.
  2. maximum circulating beam amplitude increases.
  3. inefficiency [extracted emittance] decreases [increases].
- For fixed δ, x_{sep}, and increasing $\chi/2$:
  1. octupole field strength required increases.
  2. maximum circulating beam amplitude increases.
  3. inefficiency [extracted emittance] decreases [increases].
- For fixed x_{sep}, $\chi/2$, and decreasing δ:
  1. octupole field strength required decreases.
  2. maximum circulating beam amplitude increases.
  3. inefficiency [extracted emittance] increases [decreases].

Application to the Main Injector

Constraints specific to the Main Injector eliminate most of the parameter sets listed in Tables 1-3:

- The octupole field λ is generated nearly entirely by the octupole component of the 84" quadrupoles in the ring and the 0^{th}-harmonic octupoles. The integrated field of an 84" quad at 120 GeV is $B'''L/B_0\rho = 0.450m^{-3}$. With the average value $< \beta^2 >^{1/2} \approx 56.5m$, the contribution to λ [eqn.(6)] from the 64 F quads is $\approx 150m^{-1}$. A harmonic octupole operating at its peak current of 10A generates a field $B'''L/B_0\rho = 0.418m^{-3}$. With $< \beta^2 >^{1/2} \approx 51.5m$ the 54 octupoles contribute at most $\lambda \approx 100m^{-1}$. Therefore, an acceptable value for λ is limited to the range:

$$\lambda \leq 250m^{-1} \tag{32}$$

- The extraction Lambertsons at MI-40, MI-52, MI-60, and MI-62 reduce the available horizontal aperture at those locations to roughly half the beampipe width of 5". An acceptable range for a_{max} is therefore:

$$a_{max} \leq 32mm \tag{33}$$

Finally, if it is decided (somewhat arbitrarily) that extraction inefficiency should not exceed 3%, then, of the 81 entries in Tables 1-3, only the 8 parameter sets listed in Table 4 below meet the specified criteria.

Tune Separation δ = 0.020

Septum Offset = 16.0 mm				
$\chi/2^0$	λ m^{-1}	a_{max} mm	$\pi\epsilon_N$ π-mm-mr	f %
50.	215	28.2	15.6	2.90
55.	239	29.4	20.0	2.60
Septum Offset = 18.0 mm				
45.	149	30.5	15.2	2.89
50.	170	31.7	19.8	2.58

Tune Separation δ = 0.015

Septum Offset = 16.0 mm				
$\chi/2^0$	λ m^{-1}	a_{max} mm	$\pi\epsilon_N$ π-mm-mr	f %
65.	224	30.1	16.6	2.76
70.	235	31.5	20.5	2.50
Septum Offset = 18.0 mm				
55.	152	31.2	13.4	3.00

Tune Separation δ = 0.010

Septum Offset = 14.0 mm				
$\chi/2^0$	λ m^{-1}	a_{max} mm	$\pi\epsilon_N$ π-mm-mr	f %
90.	235	31.0	14.1	2.86

Table 4: Entries from Tables 1-3 consistent with the requirements: $\lambda \leq 250m^{-1}$, $a_{max} \leq 32mm$, and $f \leq 3.0\%$.

Calculation *vs* Computation

It is time to confront the preceding predictions with numerical tracking results to determine if the effort has been at all worthwhile. In the current incarnation of the Main Injector the 53^{rd}-harmonic is excited by 8 alternately F and D quads at locations #206,208,210,212, and #506,508,510,512. This distribution produces a phase angle $\chi/2 \approx 70^0$ at the MI-52 septum. The 0^{th}-harmonic is generated by octupoles at the 54 focussing sextupole locations plus the octupole component of the MI 84" quads. A harmonic octupole kick of $0.385m^{-3}$, augmented by the kick provided by the 84" quads generates a net field of $\lambda \approx 235m^{-1}$. Selecting an initial tune separation $\delta = .015$ and septum offset of 16mm, the predicted values for a_{max}, $\pi\epsilon_N$, and f can be found in Table 4.

The numerical code[2] employed in the slow extraction simulation tracks particles via transfer matrices through drifts, dipoles, and quadrupoles, while higher multipoles are treated as kicks by zero-length elements. Field errors and misalignments are not included. The simulation proceeds as follows: the horizontal tune is raised to 26.485 and 1000 particles are randomly selected from a 30π Gaussian-distributed transverse phase-space. During the first 250 turns the harmonic octupoles and quadrupoles are ramped to $.385m^{-3}$ and $3.75(-4)m^{-1}$, respectively. At this point 30π emittance particles are marginally stable. Extraction occurs during the subsequent 1000 turns by ramping the harmonic quads to $4.65(-4)m^{-1}$, which moves the half-integer stopband through the beam.

Tracking results for the extraction parameters are compared with calculated values in Table 5. In Fig.4 the circulating beam phase-space sampled near the end of extraction is shown overlaid on the calculated separatrices. Fig.5 shows the (normalized) extracted emittance accumulated over the extraction cycle.

Method of Solution	a_{max} mm	$\pi\epsilon_N$ π-mm-mr	f %
Calculated	31.5	20.5	2.50
Tracking	32.3	23.2	2.34

Table 5: Comparison of calculated and computed extraction parameters for $\chi/2 = 70^0$, $\lambda = 235m^{-1}$, $\delta = .015$, and $x_{sep} = 16$mm.

[2]J.A. Johnstone; unpublished, undocumented, unavailable, and 'read' protected.

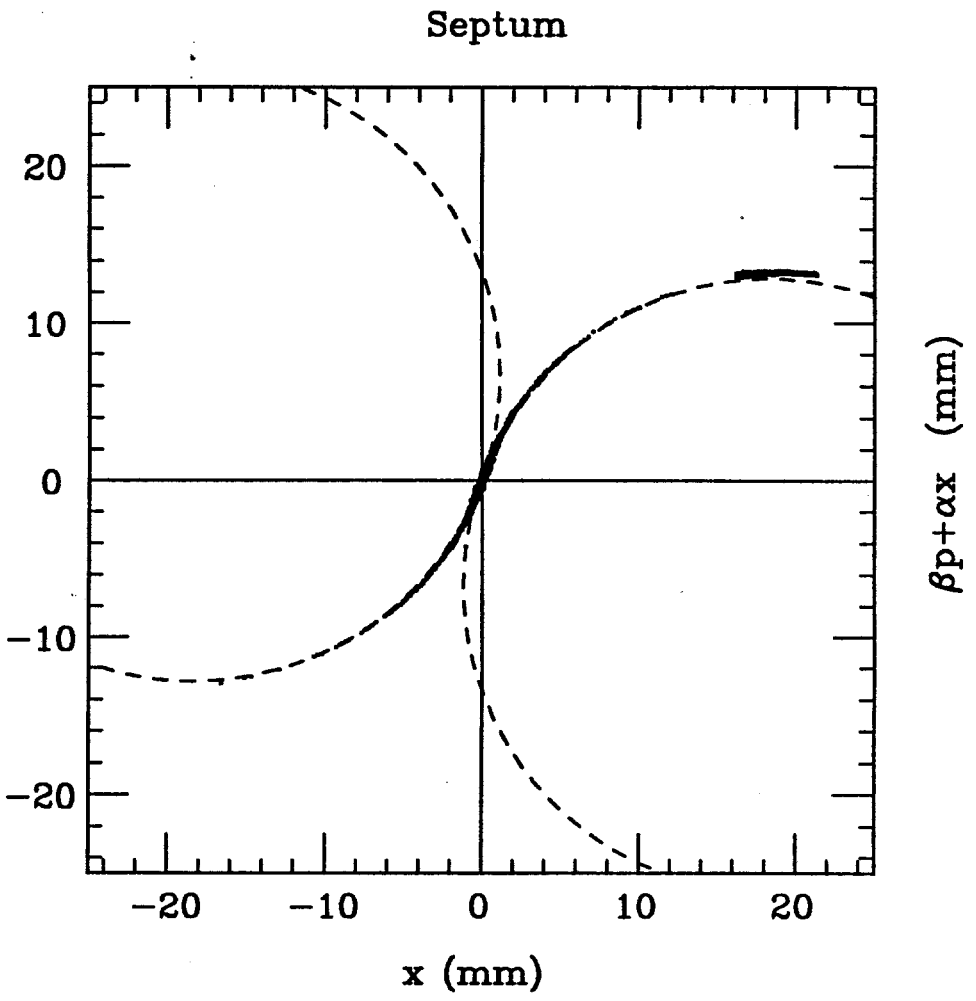

Figure 4: Circulating beam phase-space near the end of extraction. Tracking results (dots) are compared with the predicted separatrices (dashes). The high density of particles in the region $x \geq x_{sep}$ is the extracted beam accumulated over the entire cycle.

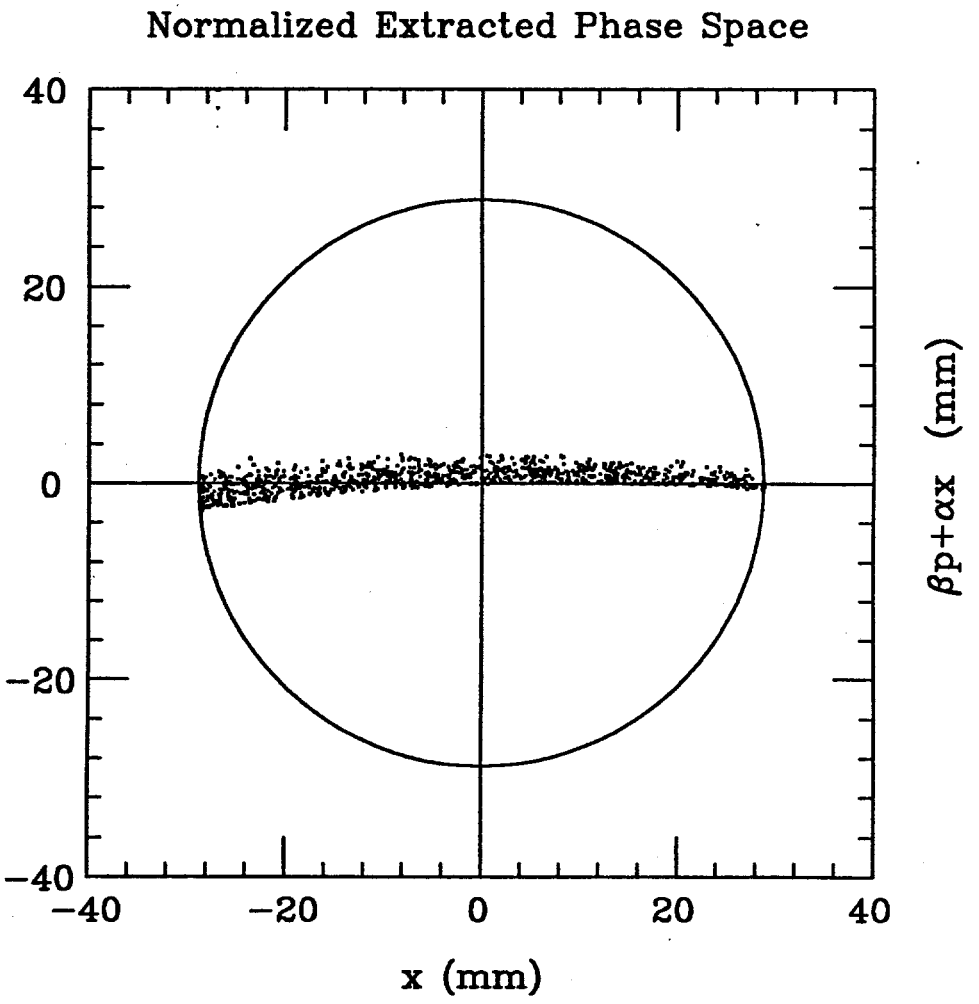

Figure 5: Enlargement from Fig.4 of the (normalized) extracted beam emittance defined by the 1000 particles extracted during the slow-spill cycle.

From Table 5: the tracking result for $\pi\epsilon_N$ is $\approx$ 13% larger than calculated, whereas inefficiency is $\approx$ 7% smaller. It is clear from eqns.(21) and (24) that this implies the step-size is $\approx$ 7% larger than anticipated. Furthermore, from Figs.4 and 5, it is apparent that, while there is good agreement between simulated and analytic phase-spaces at small amplitudes, for $x \geq x_{sep}$ the simulated phase-space deviates slightly from the analytic circle.

These discrepancies are due primarily to the true nature of the octupole field in the ring. The analytic predictions assumed that octupoles drove purely the 0^{th}-harmonic. In reality the octupole distribution also produces a small quarter-integer driving term (the two-fold symmetry of the Injector precludes a half-integer term). This additional octupole contribution is relatively unimportant at small amplitudes (quadrupole-dominated), but at large amplitudes (octupole-dominated) slightly perturbs the 0^{th}-harmonic predictions.

Conclusions

It has been shown that the simple analytic description of resonant extraction dynamics leads to predicted extraction properties that are in good agreement with results obtained from numerical simulation. Consequently, the analytic model provides the appropriate basis for initially narrowing the range of acceptable extraction parameters. It is only at this juncture, when further refinement to extraction system details requires adding field errors, misalignments, etc., to the lattice description, that numerical tracking codes become necessary tools.